Electrokinetic and Direct Force Measurements between Silica and Mica Surfaces in Dilute Electrolyte Solution

ARTICLE *in* LANGMUIR · APRIL 1997

Impact Factor: 4.46 · DOI: 10.1021/la960997c

Electrokinetic and Direct Force Measurements between Silica and Mica Surfaces in Dilute Electrolyte Solutions

Patrick G. Hartley,* Ian Larson, and Peter J. Scales

Advanced Mineral Products Special Research Centre, School of Chemistry, University of Melbourne, Parkville, Victoria 3052, Australia

Received October 15, 1996. In Final Form: January 30, 1997[⊗]

An atomic force microscope has been used to study the forces between a silica sphere in the colloidal size range and silica or mica flat surfaces as a function of distance of separation. At low ionic strength, independent electrokinetic measurements (ζ potentials) of both the spheres (by electrophoresis) and flat surfaces (by streaming potential) under the same conditions show excellent agreement with the diffuse double layer potentials derived from the force data using conventional DLVO theory. At higher ionic strength, the electrokinetically derived potentials were found to deviate from those derived from the fitted atomic force microscopy data, and a short range steric type repulsion was observed between the surfaces, the magnitude of which increased with decreasing pH.

Introduction

The properties of silica dispersions continue to present an intriguing problem to the colloid and surface chemist. In the past 30 years a multitude of electrokinetic measurements have been performed in aqueous media of various compositions which indicate a decrease in magnitude of the negative ζ potential of silica with pH toward an isoelectric point (iep) around 2−3. This has been attributed to the dissociation equilibria of surface silanols and, presumably, their eventual neutralization at low pH.[1−4] In a colloidal suspension of silica at the iep, therefore, with the electrostatic repulsions removed/minimized, one would expect rapid coagulation due to attractive van der Waals interactions. For silica sols at high electrolyte concentrations at least, this appears not to be the case, with the critical coagulation concentration of electrolyte being far higher than expected.[5,6]

A variety of direct measurements have been made of the interaction forces between silica surfaces in aqueous electrolytes.[7−17] Most of these have concentrated on attempting to gain an understanding of the short range (<10 nm) interactions operating between the surfaces, with a view to explaining the behavior of aqueous silica dispersions outlined above. The standard approach has been to measure the forces between the surfaces in a known electrolyte concentration, fit the data at large separations using various DLVO predictions, and observe deviations from these predictions at small separations. To focus on these shorter range forces, it has been usual to add electrolyte to try to eliminate the longer range electrostatic double layer repulsion and leave only the short range forces. This, however, reduces the range of the double layer force, not its magnitude. Reduction in the magnitude of the electrostatic interaction is better achieved by reducing the ζ potential. Another way of adjusting diffuse layer potentials is by the adsorption of polyvalent cations. Meagher[17] performed force measurements between a glass colloid and an oxidized silicon wafer and showed that incubation in $CaCl_2$ at pH values above 5.3 removes the short range repulsion between the surfaces, causing a strong attraction albeit at relatively high ionic strength (0.01 M). However, as outlined above, electrokinetic studies of silica colloids and surfaces have shown that the magnitude of the ζ potential is tunable quite simply by small adjustments of pH. Indeed, changes in magnitude of the order of 25 mV per pH unit are expected.[18]

In this paper we discuss the effect on force measurements of variations in pH at low ionic strength, initially as a means of assessing correlation with electrokinetic measurements but also as a method to enhance understanding of the shorter range interactions operating between the surfaces.

Experimental Section

Materials. Colloidal silica in the size range 4−6 μm was obtained from Allied Signal, Illinois. Preparation was by a modified Stöber process.[19] The colloid sample was soxhlet washed in Milli-Q water for approximately 72 h prior to use. X-ray photoelectron spectroscopy (XPS) measurements (performed by Thomas Gengenbach, CSIRO Division of Chemicals and Polymers, Australia) showed the colloid sample to be pure silica. Measurements using a nitrogen adsorption apparatus indicated that the surface area of the sample was 0.7 ± 0.1 m^2/g. Assuming a monodispersed spherical radius of 2.4−2.6 μm and a density for amorphous silica of 2.2 g/cm^3,[20] we obtain a theoretical surface area for nonporous hard spheres of 0.5−0.6 m^2/g. This indicates

* Author to whom correspondence should be addressed. E-mail: P.Hartley@chemistry.unimelb.edu.au.

⊗ Abstract published in *Advance ACS Abstracts,* March 15, 1997.

(1) Iler, R. K *The Chemistry of Silica*; Wiley: New York, 1979.
(2) Li, H. C.; DeBruyn, P. L. *Surf. Sci.* **1966**, *5*, 203.
(3) Wiese, G. R.; James, R. O.; Healy, T. W. *Discuss. Faraday Soc.* **1972**, *52*, 1438.
(4) Scales, P. J.; Grieser, F.; Healy, T. W. *Langmuir* **1992**, *8*, 965.
(5) Allen, L. H.; Matijevic, E. *J Colloid Interface Sci.* **1969**, *31* 287.
(6) Healy, T. W. In *The Colloid Chemistry of Silica* ACS Advances in Chemistry Series No. 234; Bergna, H. E. Ed.; American Chemical Society: Washington.
(7) Horn, R. G; Smith, D. T.; Haller, W. *Chem. Phys. Lett.* **1989**, *162*, 404.
(8) Peschel, G.; Belouschek, P.; Muller, M. M.; Muller, M. R.; Konig, R. *Colloid Polym. Sci.* **1982**, *260*, 444.
(9) Chapel, J.-P. *Langmuir* **1994**, *10*, 4237.
(10) Vigil, G.; Xu, Z.; Steinberg, S.; Israelachvili, J. N. *J Colloid Interface Sci.* **1994**, *165*, 367.
(11) Grabbe, A.; Horn, R. G.; *J Colloid Interface Sci.* **1993**, *157*, 375.
(12) Chapel, J.-P. *J Colloid Interface Sci.* **1994**, *162*, 517.
(13) Ducker, W. A.; Senden, T. J.; Pashley, R. M. *Nature* **1991**, *353*, 239.
(14) Ducker, W. A.; Senden, T. J.; Pashley, R. M. *Langmuir* **1992**, *8*, 1831.
(15) Butt, H.-J. *Biophys. J.* **1991**, *60*, 1438.
(16) Rabinovich, Y. I.; Derjaguin, B. V.; Churaev, N. *Adv. Colloid Interface Sci.* **1982**, *16*, 63.
(17) Meagher, L.; *J Colloid Interface Sci.* **1978**, *152*, 293.
(18) Healy, T. W.; White, L. R. *Adv. Colloid Interface Sci.* **1978**, *9*, 303.
(19) Barder, T. J.; DuBois, P. D. US Patent No. 4,983,369 Jan 1991.
(20) *CRC Handbook of Chemistry and Physics*, 75th ed.; Chemical Rubber Co.: Boca Raton, FL, 1995.

S0743-7463(96)00997-3 CCC: $14.00

that the particles are essentially nonporous, in line with the claims made in ref 19. We note that this is in contrast to many similar measurements using Stober silicas.[1] The particles were not heat treated during the experiments.

Suprasil grade fused silica flats used in both atomic force microscopy (AFM) and streaming potential experiments were polished to optical smoothness and obtained from H. A. Groiss Ltd. AFM imaging of the surfaces indicated a root mean square roughness of <2 nm over 14 μm^2. XPS measurements were performed on the flats as obtained from the manufacturer. Adventitious carbon was detected, with the only other contaminant detected being 0.2% cerium. This likely arises from the polishing process, which involves cerium oxide. In order to remove this, the plates were cleaned by soaking for 12 h in concentrated HNO_3. Immediately prior to use, the surfaces were rinsed and boiled in Milli-Q water for 20 min, then boiled for 10 min in ammoniacal H_2O_2, rinsed thoroughly again, and mounted in the AFM in a laminar flow clean air hood.

Muscovite mica was freshly cleaved prior to mounting in the AFM in a laminar clean air flow hood.

Water was Milli-Q grade, with the measured conductivity not less than 18.2 MΩ cm. Electrolytes were analytical grade reagents and were used without further purification

Methods. *AFM Force Measurements.* A Nanoscope IIIa AFM was used in the force measuring experiments and was from Digital Instruments (Santa Barbara, CA).

Gold-coated silicon nitride cantilevers used in the AFM experiments were obtained in wafer form from Digital Instruments. Several cantilevers were selected from different regions of the wafer and their spring constants determined by the method of Cleveland *et al.*,[21] which relies on monitoring the shifts in resonance frequency as a function of known attached masses to the cantilevers. The reproducibility of spring constants determined in this way was ±15% across the wafer. Cantilevers used in this study had spring constants in the range 0.03−0.20 N/m.

Cantilevers were modified for force measurements by attaching colloidal probes (in this case 5 μm diameter silica spheres) at the apex of AFM cantilevers using an extremely small quantity (1×10^{-15} L) of either 24 h curing Araldite epoxy resin or Epikote 1004. No difference was found between results obtained using the different adhesives. However, Araldite was used in the majority of the measurements as the weak cantilevers used in this study were found to deform when heated. Scanning electron microscopy indicated that the glue was always confined to the interface between the sphere and the cantilever (i.e., no contamination of the surface force sensitive region was observed). The radius of the spheres used in each experiment was measured using a light microscope to an accuracy of ±0.14 μm. Mounted colloid probes were rinsed in ethanol and dried in a filtered nitrogen stream prior to force measurement.

A detailed description of the use of the AFM in force measuring mode is provided elsewhere.[14] Briefly, the surface is ramped toward the colloid probe, and deflection of the known spring constant cantilever is measured using a laser reflected off the cantilever onto a position sensitive photodiode. Zero separation is defined from the force profile as the onset of the "constant compliance" region, where the deflection of the cantilever is linear with respect to surface displacement. Surface separation is estimated from the displacement of the lower surface relative to this constant compliance region. The force acting between probe and surface is simply determined from the deflection of the cantilever by invoking Hooke's law, $F = kD$, where D represents the deflection and k the spring constant of the cantilever.

Force separation profiles obtained using the AFM were analyzed using AFM analysis V2 software, obtained from Professor D. Y. C. Chan, Department of Mathematics, University of Melbourne. This Windows-based software allows the conversion of the raw Nanoscope force data files into force separation profiles using the user-entered parameters of spring constant and sphere radius and automatic linear fitting of the constant compliance region and zero force baseline. Theoretical DLVO force curves for similar and dissimilar surface interactions may also be generated for 1:1 electrolytes employing user-entered parameters of electrolyte concentration and diffuse layer potential.[22,23]

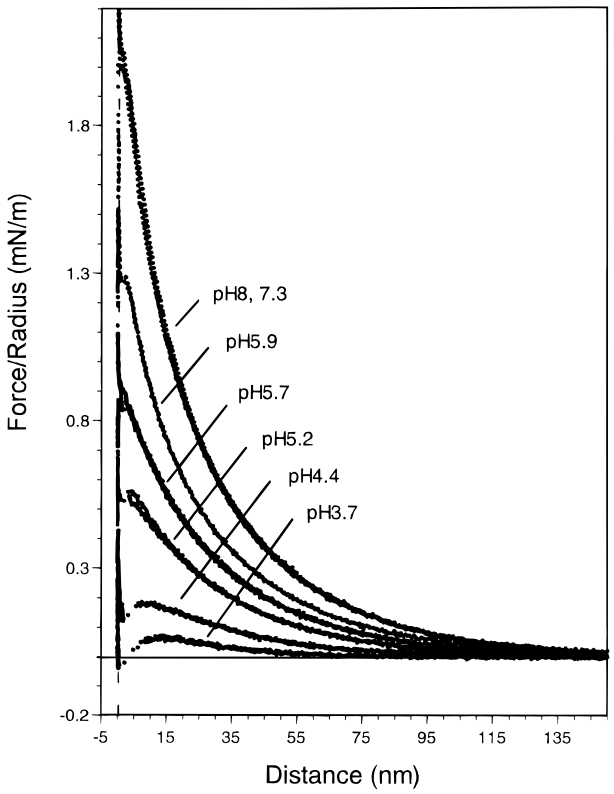

Figure 1. Measured force as a function of distance from "hard wall" compliance for interactions between a ≈5 μm silica colloid and suprasil plates in 10^{-4} M $NaNO_3$ as a function of pH.

Streaming Potential Measurements. The streaming potential apparatus was based on the design of Van Wagenen as modified by Scales et al.[4] Its operation is described in detail elsewhere.[4] Streaming potential (ΔV) was related to ζ potential using the Smoluchowski equation[24]

$$\zeta = \frac{\eta\lambda}{\epsilon_0\epsilon_r}\frac{\Delta V}{\Delta P}$$

where ΔP represents the pressure drop across the capillary formed between the surfaces of interest, λ is the conductivity of the capillary, and ϵ_0 and ϵ_r, the permittivity of free space and relative permittivity, respectively.

Microelectrophoresis Measurements. Electrophoretic velocities (v_e) were measured using a Rank Bros Mark II electrophoresis unit. The dimensions of the colloids allowed calculation of zeta potentials using the Helmholtz−Smoluchowski equation (in SI units)[25]

$$\zeta = \frac{\eta}{\epsilon_0\epsilon_r}\frac{v_e}{E}$$

where η represents the viscosity of the medium, E is the electric field strength, and ϵ_0 and ϵ_r are the permittivity of free space and relative permittivity, respectively. The electrophoretic measurements were conducted at 25 °C.

(21) Cleveland, J. P.; Manne, S.; Bocek, D.; Hansma, P. K. *Rev. Sci. Instrum.* **1993**, *64*(2), 403.

(22) Chan, D. Y. C.; Pashley, R. M.; White, L. R. *J Colloid Interface Sci.* **1980**, *77*, 283.

(23) McCormack, D.; Carnie, S. L.; Chan, D. Y. C. *J Colloid Interface Sci.* **1995**, *169*, 177.

(24) Hunter, R. J. *Zeta Potential in Colloid Science;* Academic Press: London, 1988; p 67.

(25) Hiemenz, P. C. *Principles of Colloid and Surface Chemistry*, 2nd ed.; Dekker: New York, 1986; p 751.

Results

Silica−Silica. *(1) Long Range Behavior.* Figure 1 shows force versus separation profiles between a silica colloid probe and Suprasil silica flat as a function of pH in 1×10^{-4} M sodium nitrate solutions. The force curves are characterized by an exponentially decreasing repulsive component at separations greater than 2−6 nm, while at smaller separations a strong attraction dominates the interaction, the gradient of which overcomes the spring constant causing the surfaces to jump together (note that in most cases the microscope continues to record data during the jump together, but these data are by definition nonequilibrium and should thus be ignored). The jump distance was found to decrease with increasing pH, and at pH 8.8 no inward jump was detectable. Instead, the surfaces moved abruptly from exponential repulsive to hard wall (constant compliance) behavior. Further compression of the surfaces after this jump resulted in little if any (<1 nm) inward displacement prior to the constant compliance (estimated zero separation) region of the force profile.

For pH values between 7.3 and 9.4, the magnitude and distance dependence of the long range exponential component of the interaction were invariant. At lower pH values however, the magnitude of the repulsion decreased with decreasing pH. The decay length of the interactions remained constant between pH values of 4.4 and 9.4. At pH 3.7, a slight decrease in decay length was observed. This may be explained by an increase in the effective electrolyte concentration due to the significant quantity of H^+ ions present in solution at this lower pH. This increased concentration leads to compression of the double layers adjacent to the surfaces and, hence, the observed reduction in the decay length of the interactions between the surfaces.

Analogous behavior was observable in 10^{-3} M sodium nitrate solutions as shown in Figure 2. Three notable differences between the results of Figures 1 and 2 should be highlighted:

(i) In 10^{-4} M $NaNO_3$ the plateau potential at high pH was larger in magnitude than that in 10^{-3} M electrolyte.

(ii) The decay length of the interaction at high pH was constant with respect to pH but decreased with increasing electrolyte concentration.

(iii) After the jump into contact in 10^{-3} M $NaNO_3$, the inward displacement prior to constant compliance following compression of the surfaces was somewhat larger at lower pH (1−2 nm). This phenomenon is discussed in detail later.

Excluding point (iii) for the moment, the shape and electrolyte sensitivity of the interactions between the surfaces are entirely consistent with a standard DLVO interpretation of the surface forces acting between them, and in Figure 3 we show the result of data fitting using DLVO parameters generated by the AFM Analysis 2.0 program at the two electrolyte concentrations and at high pH. The fits show that the decay length change in the exponential component of the interactions is consistent with the 10-fold difference in electrolyte concentration between the two data sets.

Repeating this fitting procedure for the remaining data in Figures 1 and 2 allows a set of theoretical diffuse layer potentials (ψ_{AFM}) to be generated for the surfaces under different conditions. The result of this fitting procedure for these and other data sets is shown in Figure 4.

We note that in none of the force profiles was a short range repulsion observed to dominate the short range jump into contact of the two surfaces. This is somewhat surprising considering measurements by several other authors which, in the majority of cases, show no attractive component to the force law between silica surfaces in similar solution conditions.[7−16]

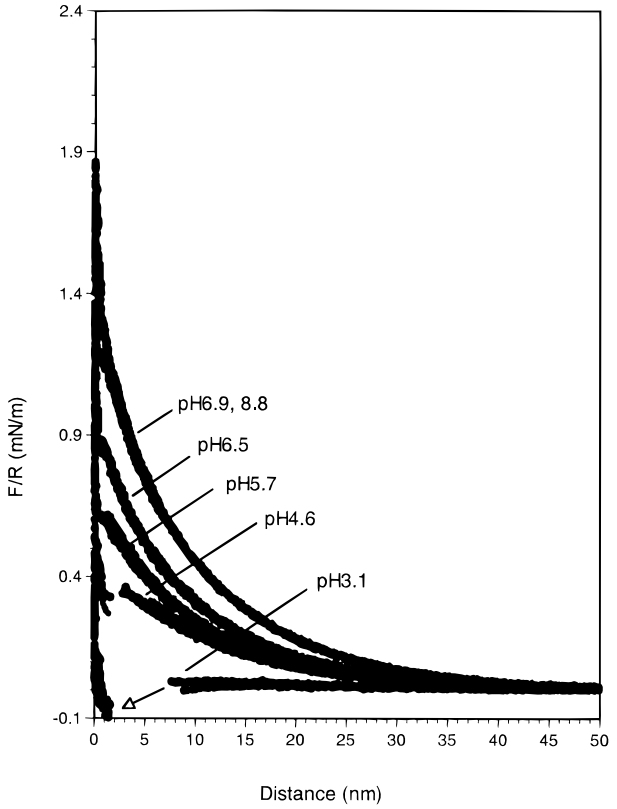

Figure 2. Measured force as a function of distance from "hard wall" compliance for interactions between a ≈5 μm silica colloid and Suprasil plates in 10^{-3} M $NaNO_3$ as a function of pH.

The trends in the data from Figure 4 suggest an isoelectric point for these surfaces at pH 2.8, which is in good agreement with previous electrokinetic data which place the iep in the range 1.8−2.8.[1−5] The linear portion of the 10^{-4} M data further suggests a change in potential per pH unit ($d\psi$/dpH) of 25 mV. This is also consistent with earlier electrokinetic studies.[3,4]

(2) Short Range Forces. The "anomalous" behavior of silica dispersions is well documented.[1,6] The data seem to indicate extra non-DLVO repulsive forces present between silica particles at low pH and high salt conditions. Various authors have attributed this to a "sterically stabilizing" or "gel layer" of polymeric silicates formed by solubilization and re-adsorption or swelling of such species from the colloid surface.[6,10,26,27] Support for this argument comes from measurements of titratable surface charge, which have often exceeded the densities possible for charge groups on a purely nonporous surface.[26,27]

An opposing argument is that water "structures" adjacent to the silica surface due to strong compatible hydrogen bonding of water with surface silanol groups. This structured water is argued to present a steric barrier to coagulation.[5,7,9,11] Either argument can be invoked to explain the short range repulsions measured between different silica surfaces in many force measurement systems.[7,9−16]

The nature of the counterion also appears to be an important mediator of coagulation and electrokinetic behavior. As has been shown in a number of studies, the

(26) Tadros, Th. F.; Lyklema, J. *Electroanal. Chem. Interfacial Electrochem.* **1968**, *17*, 267.

(27) Yates, D. E.; Healy, T. W. *J Colloid Interface Sci.* **1976**, *55*(1), 9.

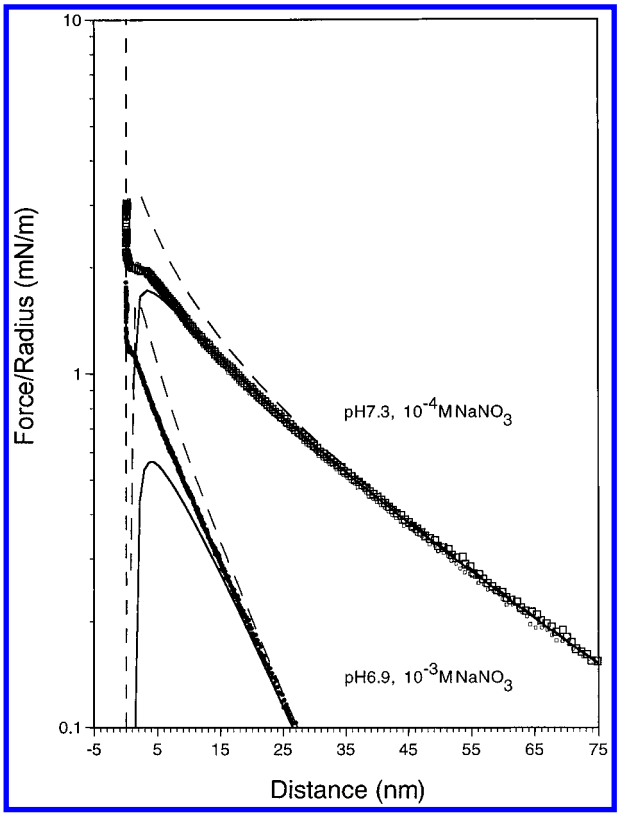

Figure 3. Sample fits to data sets from Figures 1 and 2 using the boundary conditions of constant surface charge and constant surface potential. The fitting parameters for the two data sets assume identical surface potentials for the sphere and plate at infinite separation of −105 mV, and −42 mV, and 1:1 electrolyte concentrations of 8.5×10^{-5} M (actual concentration 1×10^{-4} M) and 8.5×10^{-4} M (actual concentration 1×10^{-3} M), respectively.

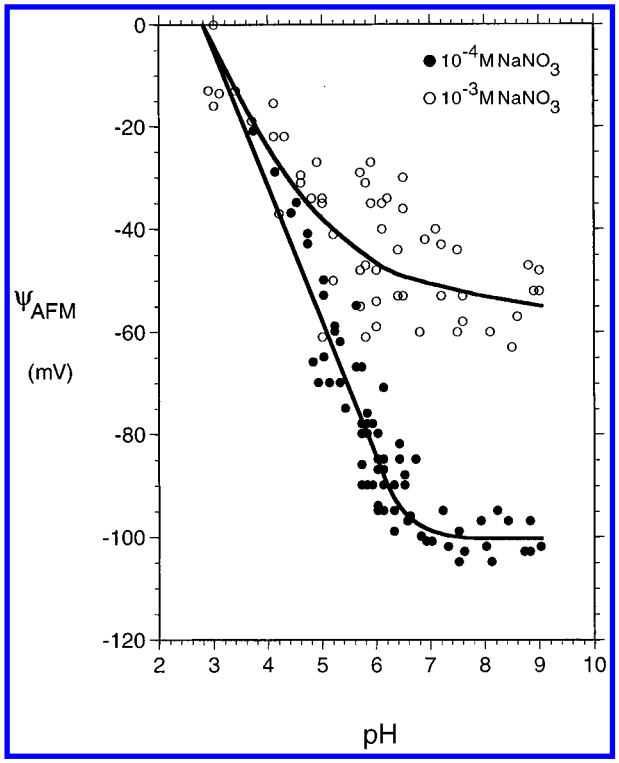

Figure 4. Results of fitting diffuse double layer potentials to silica−silica force data as a function of pH in both 10^{-4} and 10^{-3} M $NaNO_3$. The solid lines are approximate fits to the data to highlight trends.

stability of silica sols to coagulation relates to the Hofmeister series of hydrated ion size ($Li^+ > Na^+ > K^+ > Cs^+$). At high pH, the more hydrated the counterion associated with the surface, the less stable the silica sol is to coagulation. These effects have been rationalized as either differences in ability of the different ions to associate with surface and/or "gel layer" silanol groups causing lower dissociation[26,28] or, in the alternative argument, hydrated ions disrupting water structure close to the surface[5,8,9,12]

In Figure 5 we show the effect of decreasing the pH of the medium between three different samples toward their expected isoelectric point at pH 2.5. As expected, at this pH the exponential repulsive interaction was completely removed and replaced by a short range attraction originating 15 nm away from the constant compliance (putative zero separation) region of the force profile. The gradient of the attraction overcomes the spring constant at ∼8 nm separation, and the surfaces jump to a putative separation of ∼3−5 nm. Further compression was required to push the surfaces into constant compliance (0 nm). In some cases a secondary jump into compliance was observable when compression was applied. The origin of this compressible layer is unclear. Contamination seems unlikely, since the experimental apparatus and solutions are identical to those used in the previous experiments, although buildup of the layer appears to proceed only at low pH and only in the more concentrated electrolyte solutions suggesting a possible electrolyte concentration dependence. Longer range repulsions could not be induced between the surfaces using surface cleaning procedures, such as surfactant washing or UV ozone treatment.

A possible explanation is surface roughness on the sphere and/or plate, although this also seems unlikely since the same spheres and plates give hard wall contacts in different solution conditions. It is also worth noting that this behavior was not observed for silica−mica measurements performed in identical conditions discussed later. We therefore suggest that this compressible layer may be the progenitor of the polymeric silica stabilizing layers observed in the coagulation studies mentioned above. These coagulation studies were also performed at high electrolyte concentrations.

DLVO theory predicts that at the isoelectric point, interactions between identical surfaces will be dominated by a van der Waals interaction. As is shown in Figure 5, the forces predicted by a purely nonretarded van der Waals interaction (Hamaker constant = 8.5×10^{-21} J) are extremely close to those measured, but a better fit to the data is achieved by adding in a small electrostatic attraction (for simplicity retardation effects are ignored). The small amount of differing potential (±4 mV) required to fit the data implies that the potentials of the two surfaces (sphere and plate) are extremely close, perhaps surprising since they were prepared in entirely different ways. However, this provides further confidence in the assumption that the surfaces have very similar chemistries. We also note an ambiguity in the location of both the van der Waals plane and the plane of charge due to the presence of a compressible layer on the surface. For these fits, the planes of interaction have been chosen as the constant compliance region. Were the planes to be moved away from the surfaces into the compressible layer, a pure van der Waals interaction would predict the interaction more accurately, and the electrostatic attractive term could be removed.

(28) Depasse, J. Watillon, A. *J Colloid Interface Sci.* **1970**, *33*(3), 430.

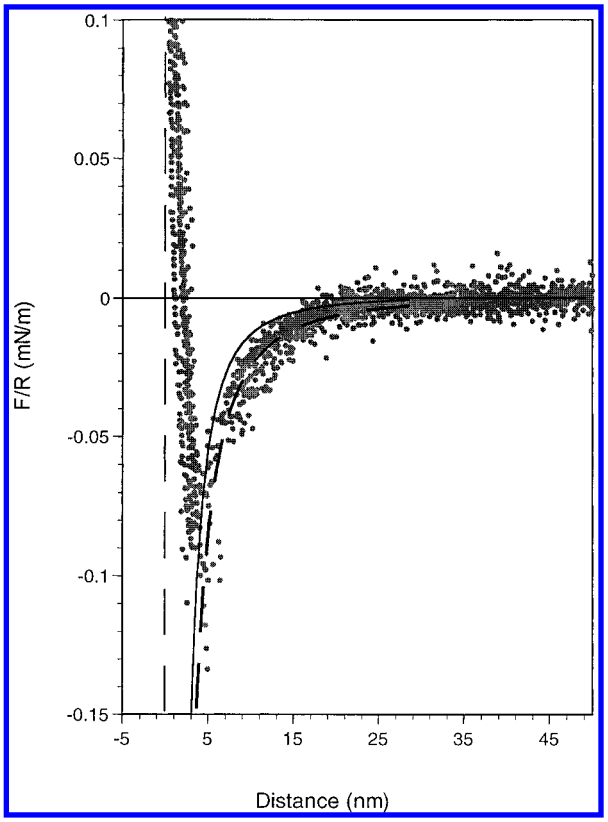

Figure 5. Forces between a silica colloid and silica flat in ≈1 × 10^{-3} M $NaNO_3$ at pH 2.2−3. The solid curve represents the theoretical prediction for a purely van der Waals interaction with a nonretarded Hamaker constant of 8.5 × 10^{-21} J. The dashed line shows the same theoretical van der Waals interaction data with an additional theoretical constant surface potential electrostatic interaction between two dissimilar surfaces bearing potentials of +4 and −4 mV, respectively, in 1 × 10^{-3} M 1:1 electrolyte.

(3) Comparison between AFM and Electrokinetic Measurements. In order to establish a firm link between conventional electrokinetic measurements and the ψ_{AFM} values from this study, it is now of interest to examine the electrokinetic properties of these surfaces. In Figure 6 we show the results of streaming potential measurements on identical Suprasil silica plates to those used in the force measurement experiment, under the same electrolyte conditions. Extrapolation of the electrokinetic data indicates an isoelectric point at pH 2.5 for the surfaces.

In Figure 7 we present the results of electrophoretic measurements obtained for identical silica colloids to those used in the force experiments. Note that these data also suggest an isoelectric point of pH 2.5. Further, the ζ potentials obtained are consistent with previous electrokinetic measurements of silica colloids.[29,30]

The similarity in the data in Figures 6 and 7 shows that the surfaces of both the colloids and surfaces used in the force experiments show similar electrokinetic behavior as a function of both pH and electrolyte concentration, which again suggests that they have very similar surface chemistries. This similarity justifies the use of a symmetric double layer fitting procedure in the AFM data analysis.

Figures 8 and 9 show the result of the comparison between fitted diffuse layer potentials derived from AFM force measurements and the electrokinetic measurements of this study. In 10^{-4} M $NaNO_3$ good agreement was

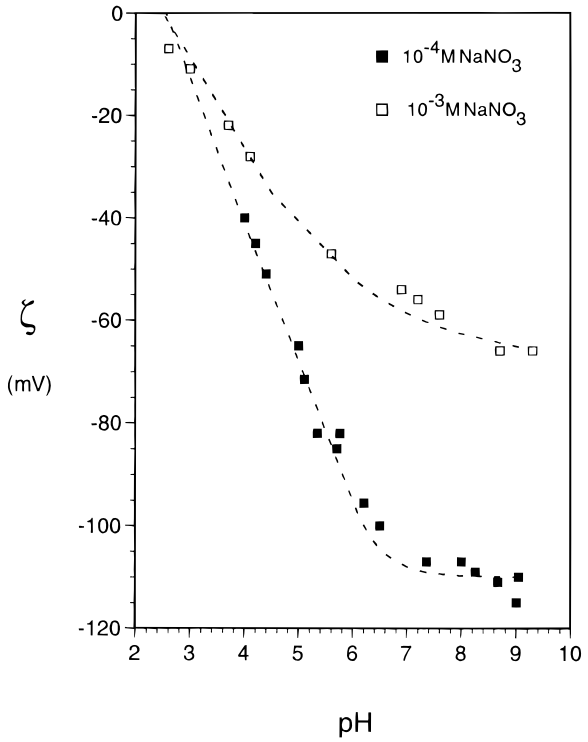

Figure 6. ζ potentials derived from streaming potential measurements in 10^{-4} and 10^{-3} M$NaNO_3$ as a function of pH for Suprasil silica flats. The dashed lines are approximate fits to the data to highlight trends.

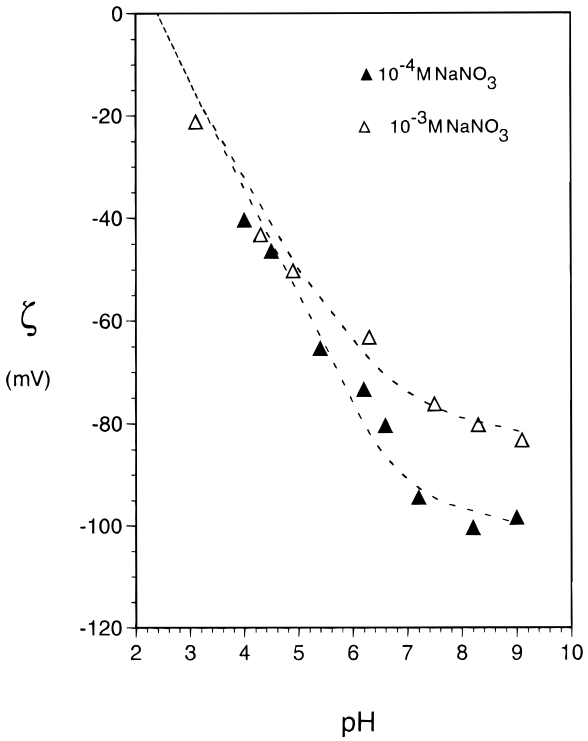

Figure 7. ζ potentials determined by electrophoresis of silica colloids in 10^{-4} and 10^{-3} M $NaNO_3$ as a function of pH. The dashed lines are approximate fits to the data to highlight trends.

obtained, with the force measurement data at higher pH values lying between the measured ζ potentials of the spheres and plates. This suggests that there is little difference between the fitted AFM diffuse layer potentials and the electrokinetic zeta potentials obtained using two independent experimental techniques at this electrolyte concentration.

(29) Abendroth, R. P. *J Colloid Interface Sci.* **1970**, *34*(4), 591.
(30) Gaudin, A. M.; Fuerstenau, D. W. *Trans AIME* **1995**, *202*, 66.

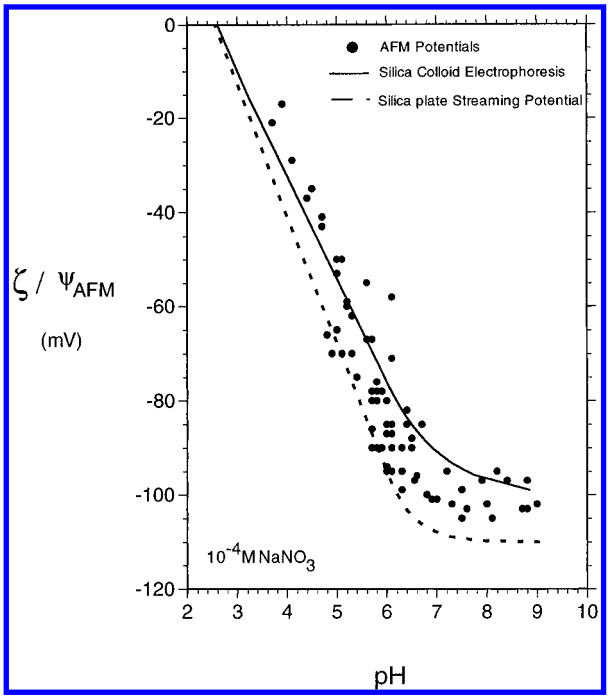

Figure 8. Comparison between approximate fits to ζ potentials and fitted AFM potentials as a function of pH in 10^{-4} M $NaNO_3$.

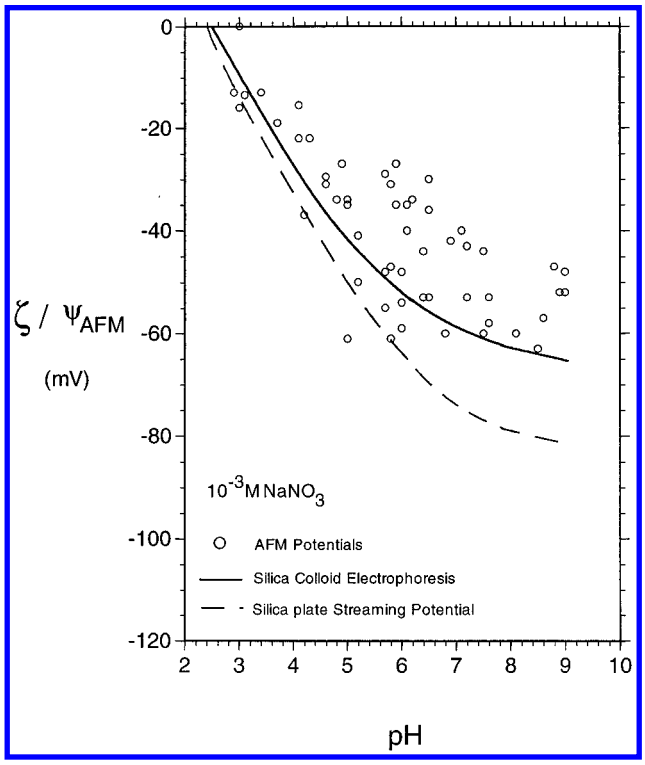

Figure 9. Comparison between approximate fits to ζ potentials and AFM potentials as a function of pH in 10^{-3} M $NaNO_3$.

The data of Figure 8 are in contrast to the data in Figure 9 for 10^{-3} M $NaNO_3$, where, for the high pH data at least, the measured AFM potentials are similar but lower in magnitude than the ζ potentials measured for the plates and considerably lower than those measured by electrophoresis of the silica colloids. A possible explanation for this discrepancy relates to the ratio of the Debye length to the root mean square roughness of the spheres and plates. At low electrolyte concentrations this ratio is large, and the roughness is insignificant compared to the double layer thickness. At higher electrolyte concentrations however, the Debye length and root mean square roughness approach each other in magnitude, and thus surface perturbations may attenuate the measured potential.

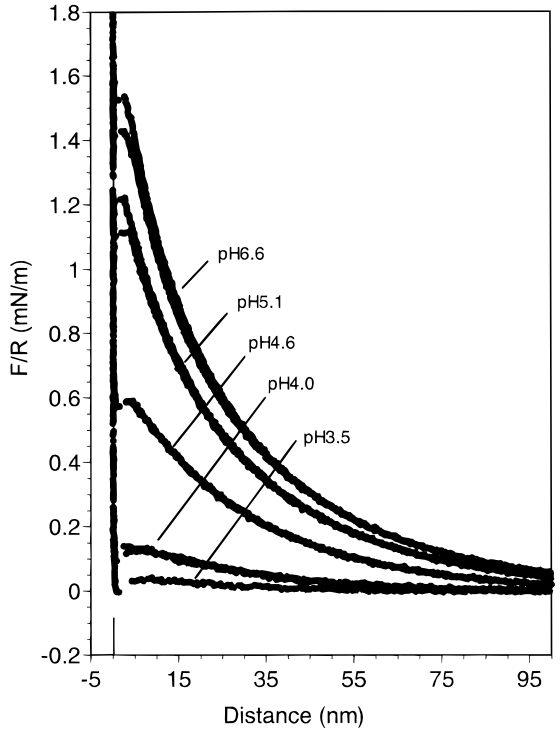

Figure 10. Measured force as a function of distance from "hard wall" compliance for interactions between a ≈5 μm silica colloid and a freshly cleaved muscovite mica surface in 10^{-4} M $NaNO_3$ as a function of pH.

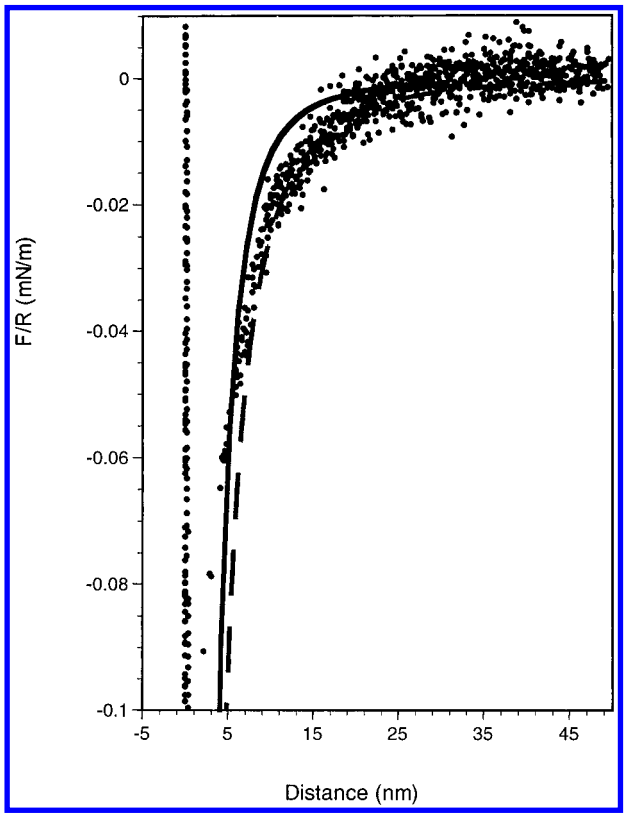

Figure 11. Forces between a silica colloid and mica surface at pH 2.5. Solid line shows a theoretical van der Waals interaction using retarded Hamaker constants (see text). The dashed line (fitting the data) shows the effect of imposing +4/−4 mV dissimilar potential on the theoretical van der Waals curve.

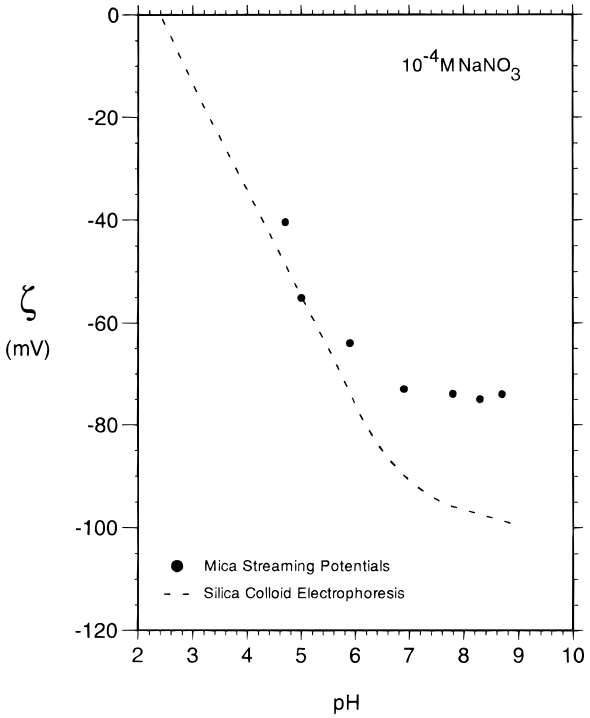

Figure 12. ζ potentials for the mica surfaces used in this study in 10^{-4} M $NaNO_3$. Data were obtained using the streaming potential apparatus. The dashed line represents the approximate fit to the ζ potential data for silica colloids in 10^{-4} M $NaNO_3$ from Figure 7.

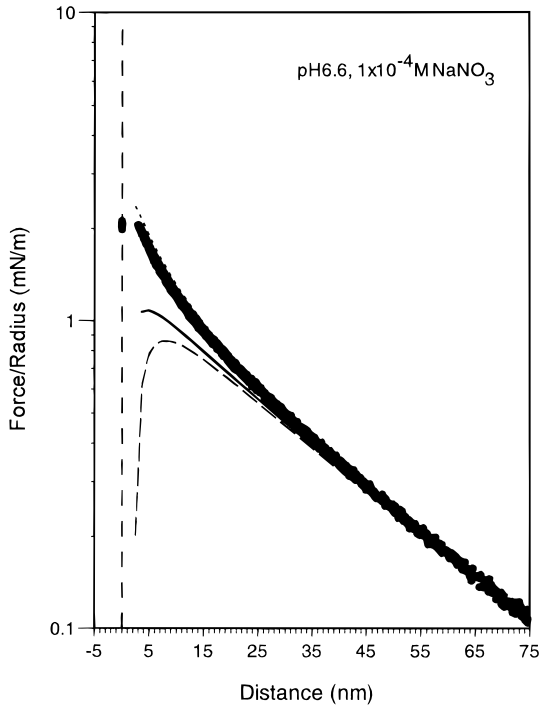

Figure 13. Dissimilar double layer fitting of force profiles recorded for silica vs mica interaction at pH 6.6 in 10^{-4} M $NaNO_3$: (——) constant surface potential model, $\zeta_{silica} = -86$ mV, $\psi_{mica} = -87$ mV, 1×10^{-4} M electrolyte; (– – –) constant surface potential model, $\zeta_{mica} = -75$ mV, $\psi_{silica} = -99$ mV, 1×10^{-4} M electrolyte; (- - -) constant surface charge model, $\zeta_{silica} = -86$ mV, $\psi_{mica} = -87$ mV, 1×10^{-4} M electrolyte; (•••) constant surface charge model, $\zeta_{mica} = -75$ mV, $\psi_{silica} = -99$ mV; 1×10^{-4} M electrolyte (obscured by data).

Silica–Mica. In Figure 10 we show force separation profiles obtained for a silica–mica interaction in 10^{-4} M $NaNO_3$. As in the case of the silica–silica interaction

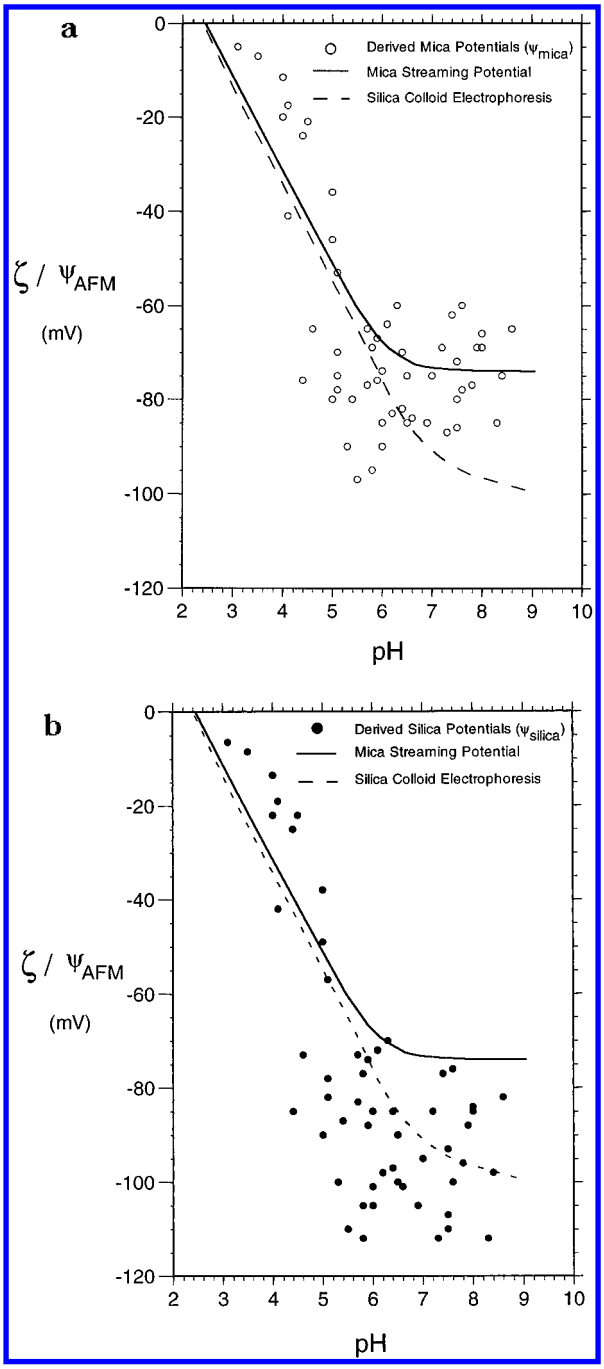

Figure 14. (a) ψ_{mica} values obtained by fitting silica–mica interactions using dissimilar double layer theory (ψ_{silica} set equal to ζ_{silica} and ψ_{mica} adjusted to fit force data). (b) ψ_{silica} values obtained by fitting silica–mica interactions using dissimilar double layer theory (ψ_{mica} set equal to ζ_{mica} and ψ_{silica} adjusted to fit force data).

profiles (Figure 1), the forces are characterized by an exponentially decreasing repulsive component at large separations which gives way to a strong attraction at small separations causing the surfaces to jump into contact. Once again the repulsive component decreases in magnitude with decreasing pH below pH 6.9.

At pH 3 (Figure 11), the repulsive component was removed, and the surfaces were attracted toward each other from a separation of approximately 20–25 nm. In this case, after the jump together, further compression did not alter the relative positions of the sphere and plate; hence no compressible layer was apparent. The theoretical retarded van der Waals interaction in this case was

calculated using optical data for both mica and fused silica[32,33] and calculated using the method described by Pashley.[34] The calculations yielded an effective non retarded Hamaker constant at zero separation of 1.2×10^{-20} J. Once again, the theoretical van der Waals interaction alone was not sufficient to fit the data adequately, and a small electrostatic attraction was invoked. As before, the magnitude of the potentials required to fit the data was low, suggesting the sphere and plate have a similar isoelectric point. This hypothesis is supported by streaming potential measurements using the same mica sample. These are shown in Figure 12. The magnitude and pH dependence of the mica zeta potential are in good agreement with earlier electrokinetic measurements.[31] Fitting of data from the surface force apparatus also gives surface potentials close to those observed at pH values close to 6.[35] At pH values less than 6.9, the mica streaming potential data agree with both the electrokinetic and force measurement values for the silica surfaces previously discussed. Above this pH limit, a plateau in ζ potential is observed at -75 mV, which is lower than that obtained for both the silica plates and colloids in the same electrolyte conditions (see Figures 6 and 7).

When AFM force data are analyzed from this dissimilar system, DLVO theory requires the input of two diffuse layer potentials, ψ_{silica} and ψ_{mica}. On the basis of the assumption that the measured ζ-potentials (Figures 7 and 12) are good approximations for these diffuse layer potentials in low electrolyte conditions, we can use them as a guide in theoretical fitting of the experimental force data. Experimental force profiles at each pH can be fitted in two ways: (i) fix ψ_{silica} at ζ_{silica} and adjust ψ_{mica} until theoretical and experimental force profiles overlap; (ii) fix ψ_{mica} at ζ_{mica} and adjust ψ_{silica} until similar agreement is achieved. Examples of these fitting procedures for data at pH 6.6 are shown in Figure 13. Performing these fitting procedures on experimental data obtained at different pH values yields two sets of pH vs ψ_{AFM} data.

In Figure 14a we present the results from fitting procedure i (i.e., fixing ψ_{silica} at ζ_{silica}; reasonable agreement is seen between the values of ψ_{mica} derived in this way and ζ_{mica} from Figure 12. Results from fitting procedure ii are presented in Figure 14b. Good agreement is also seen between the derived ψ_{silica} and ζ_{silica} from Figure 7.

Conclusions

Surface force and ζ potential measurements have been performed in a variety of conditions using vitreous silica (Suprasil) or freshly cleaved mica surfaces and a silica colloid.

Good correlation between fitted force measurements and zeta potentials has been found for the flat surfaces and colloids used in these experiments at low ionic strength. At a higher ionic strength, deviation between force measurements and ζ potentials of the silica colloids was observed; however this may reflect a dependence on surface roughness.

No short range repulsion between the silica surfaces was observed at low ionic strength, with the surfaces jumping into contact once a threshold repulsion was overcome. The apparent range of the attraction increased as the threshold repulsion was reduced, in line with DLVO theoretical predictions. This indicates that in this case surface hydration/gelation was not able to overcome the van der Waals attraction between the surfaces as has been suggested previously.

At higher electrolyte concentration and low pH, a compressible layer was observed which increased in thickness as the pH was decreased toward the isoelectric point. Force measurements made at or close to the predicted isoelectric point of the silica surfaces showed an attractive interaction which was close to that predicted by a purely van der Waals force law. The compressible layer observed between silica surfaces at higher ionic strength showed maximum thickness in these conditions; thus the existence of a counterion mediated hydration force cannot be ruled out. No such steric barrier was observed in low pH conditions for the silica−mica interaction.

Differences between this and similar studies may be attributable to the slightly different technique used in production of the colloidal spheres. The technique is reported to produce nonporous spherical silica colloids. This system provides an ideal starting point for further studies of the possible mechanism for the buildup of short range repulsions between silica surfaces.

Acknowledgment. P.G.H. acknowledges financial support from the Royal Society via a Postdoctoral fellowship. I.L. acknowledges the reciept of an Australian Postgraduate Research Award. Further financial support for the work was provided by the Advanced Mineral Products Special Research Centre, an Australian Reserch Council Special Research Centre. Thanks to James Tardio for performing the streaming potential measurements on the mica samples and to Dr. L. Meagher for calculating retarded Hamaker constants. Discussions and advice from Professor T.W. Healy and Professor D.Y.C. Chan are also gratefully acknowledged.

LA960997C

(31) Scales, P. J.; Grieser, F.; Healy, T. W. *Langmuir* **1990**, *6*, 582.
(32) Christenson, H. K.; PhD Thesis, Australian National University, Canberra, Australia, 1983.
(33) Hunter, R. J. *Foundations of Modern Colloid Science;* Clarendon Press: Oxford, 1989; Vol. I.
(34) Pashley, R. M. *J Colloid Interface Sci.* **1977**, *62*, 344.
(35) Israelachvili, J. N.; Adams, G. E. *J. Chem. Soc., Faraday Trans. 1* **1978**, *74*, 975.